Articles

Structural Evolution in Cationic Micelles upon Incorporation of a Polar Organic Dopant

Mohit Singh,[†] Christy Ford,[†] Vivek Agarwal,[‡] Gerhard Fritz,[§] Arijit Bose,[‡] Vijay T. John,*[,†] and Gary L. McPherson[||]

Department of Chemical and Biomolecular Engineering, Tulane University, New Orleans, Louisiana 70118, Department of Chemical Engineering, University of Rhode Island, Kingston, Rhode Island 02881, Institut für Chemie, Karl-Franzens Universität Graz, 8010 Graz, Austria, and Department of Chemistry, Tulane University, New Orleans, Louisiana 70118

Received April 23, 2004. In Final Form: August 8, 2004

Micelles of cetyltrimethylammonium bromide (CTAB), when doped with increasing levels of 4-ethylphenol, show microstructural transitions from spherical micelles to elongated wormlike micelles, disks, and subsequently to globular and then to tubular vesicles. Wormlike micelles are observed at a dopant-to-CTAB molar ratio of 1:3. At higher dopant ratios (1:1), globular vesicles are observed which transition to tubular vesicles when the dopant becomes the predominant species at a ratio of 3:1. These transitions are reflected in small-angle neutron scattering analysis and, interestingly, can be directly observed through cryo-transmission electron microscopy. The para-substituted phenol is interfacially active and modulates interfacial curvature of the micelles. The observations of microstructure modifications have relevance to the synthesis of mesoporous materials using CTAB as the template.

Introduction

Surfactant molecules self-assemble to form a variety of microstructures. The organization of surfactant molecules is often described by the packing parameter (g): $g = V/a_o l$, where V is the effective volume of the surfactant tail region, a_o refers to the effective headgroup area at the micelle surface, and l is the surfactant tail length.[1] Conical effective surfactant shapes that tend to pack into spherical micellar structures with high interfacial curvature result from g values less than 1/3. Increasing the value of g leads to transitions to rodlike or cylindrical micelles, to lamellar and bilayer structures, and eventually to inverse micelles with negative curvatures at $g > 1$.

Inorganic and organic salts have been widely used as dopants to facilitate the structural transition of micelles in ionic surfactant solutions.[2−5] Inorganic counterions promote gradual micellar growth by reducing the headgroup repulsions in the ionic micelles. The headgroup repulsions are reduced as the counterions bind moderately to the ionic micelles and change the ionic strength of the medium. Organic salts in aqueous micellar systems dissociate to produce ionic species with a hydrophobic moiety which affects the packing of the surfactant tails and leads to changes in the effective packing parameter.[6] The growth of cationic surfactant (cetyltrimethylammonium bromide, CTAB) micelles has been widely studied in the presence of salts such as KBr,[7] sodium salicylate,[8,9] chlorobenzoate,[10] and benzyl sulfonates.[11] Increased salt concentrations cause the microstructure to change from globular to wormlike micelles.[12,13] The discovery of the spontaneous formation of vesicles in mixtures of cationic and anionic surfactants is a particularly fascinating consequence of controlling and modulating interfacial curvature through charge interactions.[14]

The effect of nonionic dopants on micellar shape is also of interest and is the subject of this paper. Hedin and co-workers have reported the elongation of CTAB micelles upon the solubilization of benzene.[15] Zhang and co-workers investigated the effect of benzyl alcohol on CTAB/KBr micellar systems through a combination of rheology and NMR and have suggested elongation of micelles upon

* Author to whom correspondence should be addressed. E-mail: vijay.john@tulane.edu.

[†] Department of Chemical and Biomolecular Engineering, Tulane University.

[‡] University of Rhode Island.

[§] Karl-Franzens Universität Graz.

[||] Department of Chemistry, Tulane University.

(1) Israelachvili, J. N. *Intermolecular and Surface Forces*, 2nd ed.; Academic Press: New York, 1992.

(2) Mazer, N. A.; Benedek, G. B.; Carey, M. C. *J. Phys. Chem.* **1976**, *80*, 1075.

(3) Kern, F.; Lemarechal, P.; Candau, S. J.; Cates, M. E. *Langmuir* **1992**, *8*, 437.

(4) Hassan, P. A.; Raghavan, S. R.; Kaler, E. W. *Langmuir* **2002**, *18*, 2543.

(5) Khatory, A.; Lequeux, F.; Kern, F.; Candau, S. J. *Langmuir* **1993**, *9*, 1456.

(6) Buwalda, R. T.; Stuart, M. C. A.; Engberts J. B. F. N. *Langmuir* **2000**, *16*, 6780.

(7) Aswal, V. K.; Goyal, P. S. *Chem. Phy. Lett.* **2002**, *357*, 491.

(8) Hoffmann, H.; Rehage, H.; Platz, G.; Schorr, W.; Thurn, H.; Ulbricht, W. *Colloid Polym. Sci.* **1982**, *260*, 1042.

(9) Hassan, P. A.; Yakhmi, J. V. *Langmuir* **2000**, *16*, 7187.

(10) Rao, U. R. K.; Manohar, C.; Valaulikar, B. S.; Iyer, R. M. *J. Phys. Chem.* **1987**, *91*, 3286.

(11) Pal, O. R.; Gaikar, V. G.; Joshi, J. V.; Goyal, P. S.; Aswal, V. K. *Langmuir* **2002**, *18*, 6764.

(12) Porte, G.; Appell, J. *J. Phys. Chem.* **1981**, *85*, 2511.

(13) Rehage, H.; Hoffmann, H. *Mol. Phys.* **1991**, *74*, 933.

(14) Kaler, E. W.; Murthy, A. K.; Rodriguez, B.; Zasadzinski, J. A. N. *Science* **1989**, *245*, 1371. Kaler, E. W.; Herrington, K. L.; Murthy, A. K.; Zasadzinski, J. A. N. *J. Phys. Chem.* **1992**, *96*, 698.

(15) Hedin, Niklas; Sitnikov, Ruslan; Furo, Istvan; Henriksson, U.; Regev, Oren. *J. Phys. Chem. B* **1999**, *103*, 9631.

10.1021/la048967u CCC: $27.50
Published on Web 10/06/2004

alcohol solubilization.[16] The addition of alcohols has also been shown to promote growth of wormlike micelles in such transitions.[17−19]

In this paper, we report the effect of phenols, in particular of 4-ethylphenol, a polar but nonionic dopant, on the structure of cationic micelles of CTAB. Because 4-ethylphenol has a very low dissociation constant ($pK_a \approx 10$), the counterion effect is not expected to play a significant role in altering the micelle shape and size. However, the polarity of the molecule and its incorporation into the surfactant palisade layer are expected to affect the manner in which the surfactant molecules aggregate. The effect of monomer incorporation in CTAB micelles is investigated through nuclear magnetic resonance (NMR) spectroscopy, small-angle neutron scattering (SANS), and cryo-transmission electron microscopy (cryo-TEM). We report a systematic structural transition in the CTAB micelles upon incremental additions of the dopant, 4-ethylphenol. The micellar system exhibits a spherical micelles-to-elongated micelles-to-vesicles transition that can be captured through SANS. We also show corroboration of SANS results through cryo-TEM where microstructure transitions are confirmed through direct imaging.

The choice of CTAB as a model surfactant and phenol as the polar additive is also of applied interest. Cationic surfactants such as CTAB are widely investigated for their relevance to the templated synthesis of mesoporous materials.[20] The addition of organic additives to these surfactant systems could create effective methods to induce structural changes and modify mesopore geometry.[21] Additionally, the incorporation of phenol and aromatic amine monomers into micelles and inverse micelles creates confined environments for the chemical or enzymatic synthesis of novel polyphenolics and polyaromatic amines.[22,23] The coupling of such polymer synthesis with mesoporous materials synthesis can lead to novel polymer−ceramic nanocomposites.[24]

Experimental Section

Materials and Methods. CTAB, HEPES buffer, and 4-ethylphenol were purchased from Sigma-Aldrich. Deuterium oxide (99.9%) was purchased from Cambridge Isotopes Laboratory. All chemicals were used without further treatment and/or purification.

A 50 mM CTAB (2% w/w) solution was prepared using 0.1 M HEPES buffer, pH 5.3. 8.7 mM to 0.34 M 4-ethylphenol was dissolved in the CTAB micelles with the phenol-to-surfactant molar ratio (M) ranging from 0.17 to 3. The solution was stirred vigorously until the phenol was solubilized. All samples were maintained at 25 °C.

NMR. NMR measurements were performed at 25 °C on a Bruker DRX 500 MHz NMR spectrometer. All samples for NMR were prepared in D_2O.

SANS. SANS measurements were carried out on the 30 m NG3 beamline at the NIST Center for Neutron Research (NCNR, Gaithersburg, MD). The instrument utilizes a mechanical velocity selector as a monochromator, a circular pinhole collimator, and a two-dimensional position-sensitive detector (65×65 cm^2). The SANS intensity, I, was recorded as a function of the magnitude of the scattering vector q ($=4\pi \sin(\theta/2)/\lambda$), where θ is the scattering angle and λ is the neutron wavelength, equal to 6 Å). The detector angle was set at 2°, and the sample-to-detector distance was set to 2 and 13 m to cover the widest possible range of q (0.004−0.6 Å^{-1}). Samples were contained in closed stainless steel cells with quartz windows that provided a path length of 2 mm. The sample temperature was maintained at 25 °C. The raw data was corrected for the scattering from an empty quartz cell, detector sensitivity and background, and transmission of each sample and placed on an absolute scale using software provided by NCNR. The primary component in our microemulsion system is D_2O. The scattering data were plotted as $I(q) - B$ where $I(q)$ is the total scattered intensity and B is the background calculated from the slope of a Porod plot (Iq^4 versus q^4).

Cryo-TEM. Cryo-TEM is a very useful technique for analyzing microstructures in liquid samples using transmission electron microscopy. In the procedure, an ~5 μL drop of the microemulsion is first placed on a holey polymer film supported on a TEM grid. The drop is blotted by a filter paper creating a thin film (<200 nm) of the liquid over the grid, which is then placed in a controlled environment vitrification chamber (CEVS).[25] The sample is immediately vitrified in liquid ethane at its freezing temperature. The grid is transferred under liquid nitrogen to a cryo-transfer stage (Oxford Instruments CT-3500) designed for minimal air exposure and heat loss. The samples were observed using a JEOL 1200EX S/TEM, coupled with the TVIPS F-224 slow-scan CCD (2048×2048 resolution) camera at −170 °C.

Data Analysis

Two approaches for analyzing the SANS data from micellar systems involve fitting the experimental data to a known scattering model, or the use of a model-free approach.[26] The first approach is to compare the scattering data to calculated scattering curves of model structures. The limitation of this model-fitting approach is that multiple models can describe a set of SANS data through parameter adjustments, making it very difficult to find the correct model without any a priori knowledge about the scattering system.

The analysis of SANS data presented here deals with the second approach, in particular, a technique called generalized indirect Fourier transformation (GIFT) developed by Glatter and co-workers.[27,28] Generally, this procedure is preferred if there is not enough information to make any a priori assumption, especially if the scattering entities interact. The scattering intensity $I(q)$

(16) Zhang, W.-C.; Li, G.-Z.; Shen, Q.; Mu, J.-H. *Colloids Surf., A* **2000**, *170*, 59.

(17) Chiruvolu, S.; Warriner, H. E.; Naranjo, E.; Idziak, S. H. J.; Rädler, J. O.; Plano, R. J.; Zasadzinski, J. A.; Safinya, C. R. *Science* **1994**, *266*, 1222.

(18) Hoffmann, H.; Thunig, C.; Valiente, M. *Colloids Surf.* **1992**, *67*, 223. Hoffmann, H.; Munkert, U.; Thunig, C.; Valiente, M. *J. Colloid Interface Sci.* **1994**, *163*, 217. Gradzielski, M.; Bergmeier, M.; Müller, M.; Hoffmann, H. *J. Phys. Chem. B* **1997**, *101*, 1719.

(19) Oda, R.; Bourdieu, L.; Schmutz, M. *J. Phys. Chem. B* **1997**, *101*, 5913.

(20) Kresge, C. T.; Leonowicz, M. E.; Roth, W. J.; Vartuli, J. S. *Nature* **1992**, *359*, 710. Beck, J. S.; et al. *J. Am. Chem. Soc*. **1992**, *114*, 10834−10843.

(21) Lind, A.; Andersson, J.; Karlsson, S.; Agren, P.; Bussian, P.; Amenitsch, H.; Linden, M. *Langmuir* **2002**, *18*, 1380. Sayari, A.; Yang, Y.; Kruk, M.; Jaroniec, M. *J. Phys. Chem. B* **1999**, *103*, 3651. de Soler-Illia, G. J.; Sanchez, C.; Lebeau, B.; Patarin, J. *Chem. Rev.* **2002**, *102*, 4093. Yabuki, M.; Takahashi, R.; Sato, S.; Sodesawa, T.; Ogura, K. *Phys. Chem. Chem. Phys.* **2002**, *4*, 4830. Blin, J. L.; Su, B. L. *Langmuir* **2002**, *18*, 5303.

(22) Akkara, J. A.; Ayyagari, M.; Bruno, F.; Samuelson, L.; John, V. T.; Karayigitoglu, C.; Tripathy, S.; Marx, K. A.; Rao, D. V. G. L. N.; Kaplan, D. L. *Biomimetics* **1994**, *2*, 331. Premchandran, R.; Banerjee, S.; John, V. T.; McPherson, G. L.; Akkara, J. A.; Kaplan, D. L.; Ayyagari, M. *Macromolecules* **1996**, *29*, 6452. Premchandran, R.; Banerjee, S.; John, V. T.; McPherson, G. L.; Akkara, J.; Kaplan, D. L. *Chem. Mater.* **1997**, *9*, 1342.

(23) Liu, W.; Kumar, J.; Tripathy, S.; Samuelson, L. *Langmuir* **2002**, *18*, 25.

(24) Ford, C. D.; Singh, M.; McPherson, G.; John, V. T. *Colloids Surf., B*, in press (ASAP Publication on the Web).

(25) Bellare, J. R.; Davis, H. T.; Scriven, L. E.; Talmon, Y. *J. Electron Microsc. Technol.* **1988**, *10*, 87.

(26) Glatter, O. *J. Appl. Crystallogr*. **1977**, *10*, 415.

(27) Glatter, O. *J. Appl. Crystallogr*. **1981**, *14*, 577. Glatter, O.; Hainisch, B. *J. Appl. Cryst*. **1984**, *17*, 435. Glatter, O. *J. Appl. Crystallogr*. **1988**, *21*, 886.

(28) Fritz, G.; Bergmann, A.; Glatter, O. *J. Chem. Phys.* **2000**, *113*, 9733. Bergman, A.; Fritz, G.; Glatter, O. *J. Appl. Crystallogr.* **2000**, *33*, 1212.

at different scattering vectors, **q**, where

$$q = \frac{4\pi}{\lambda} \sin\left(\frac{\theta}{2}\right) \tag{1}$$

is only a function of shape, size, and internal structure for noninteracting particles. In the case of interacting particles, the intensity does not depend solely on these parameters. Neighboring particles can influence the scattering curve considerably, leading to interparticle effects represented by the so-called structure factor $S(q)$, while the intraparticle effects are described by the form factor $P(q)$. In the case of N monodisperse, homogeneous, globular, interacting particles, the total scattering intensity can be expressed by

$$I(q) = NP(q)S(q) \tag{2}$$

This factorization allows a separation of inter- and intraparticle effects by means of the GIFT technique. The GIFT method approximates the form factor, represented by a linear combination of a finite number of cubic B-spline functions. At the same time, a model for the structure factor is assumed and fitted to the data according to eq 2. This simultaneous approximation of form and structure factor is only possible due to the different mathematical properties of the two functions. Nevertheless, the problem is now highly nonlinear and has to be solved in an iterative way. Fritz and co-workers[28] have explained the steps involved in this GIFT calculation in a detailed and well-structured manner. For a particle of arbitrary shape, the pair distance distribution function (PDDF) $p(r)$ is given by

$$p(r) = r^2\Delta_\rho^{-2}(r) \tag{3}$$

where $\Delta_\rho^{-2}(r)$ is the convolution square of $\Delta\rho(r)$, the scattering density difference, averaged over all directions. The PDDF is related to the scattered intensity $I(q)$ through the form factor $P(q)$ by the Fourier transformation

$$P(q) = 4\pi\int_0^\infty p(r)\frac{\sin(qr)}{qr}\,dr \tag{4}$$

The shape of the PDDF offers a fair idea of the basic geometry, such as spherical, cylindrical, and lamellar, even for inhomogeneous particles. Knowledge of $p(r)$ also excludes certain structural alternatives. After the PDDF is determined, a cross-sectional $p(r)$ can be obtained that provides further information about the cross-sectional shape and size of the scattering entities by using the symmetry obtained in the first step.

Strictly speaking, the factorization into a form factor and a structure factor is only possible for spherical particles due to orientation correlations. But it has been shown for low concentrations that an evaluation by means of the GIFT technique is possible if the length of the particles is on the order of magnitude of the radius.[28] As stated, a model for the structure factor has to be assumed for use in the GIFT technique. Therefore, models for charged particles are necessary to extend the method to this important group of colloids. In the present study, the Ornstein−Zernike equation with hypernetted-chain (HNC) approximation for closure relation is used, which has been shown to work very well for aqueous CTAB solutions. The details of this (GIFT) technique can be found in the same reference.[28]

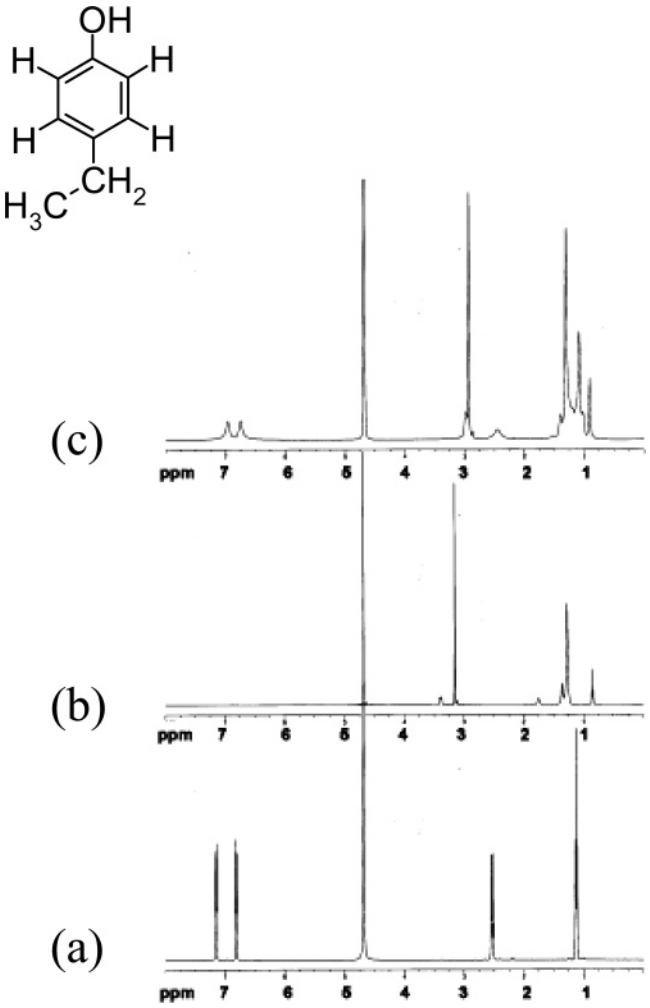

Figure 1. NMR spectra of (a) 17 mM 4-ethylphenol, (b) 25 mM CTAB, and (c) 17 mM 4-ethylphenol + 25mM CTAB in D_2O. The structure of the dopant, 4-ethylphenol, is also indicated. The peak at $\delta = 4.681$ is the residual water (H_2O) resonance since all samples contain traces of nondeuterated water.

Results and Discussion

The addition of 4-ethylphenol into CTAB micelles at 25 °C results in fully stable solutions at all dopant concentrations used in this study. At low dopant-to-surfactant molar ratios, ($M < 1$), the micellar solutions are fully transparent. At higher M values ($M = 1$ and $M = 3$), the solution becomes slightly turbid, indicating the presence of larger assemblies in the system.

The interaction of the dopant molecule, 4-ethylphenol, with CTAB micelles was studied using NMR spectroscopy. The ^{1}H NMR spectra of 4-ethylphenol were measured in the presence and absence of CTAB. Figure 1a illustrates the NMR spectrum of 17 mM 4-ethylphenol in the absence of CTAB. The two ortho protons of the aromatic ring appear as a downfield doublet ($\delta = 7.152$ and 7.136 ppm) because of coupling with the meta protons. Due to coupling with the ortho protons, the two meta protons appear as a doublet shifted upfield ($\delta = 6.820$ and 6.803 ppm). The two ($-CH_2$) protons appear as a quadruplet ($\delta \approx 2.53$) because of coupling with 3 methyl ($-CH_3$) protons. The methyl protons (coupled with $-CH_2$ protons) appear at $\delta = 1.122$. Figure 1b is the NMR spectrum of 25 mM CTAB, and Figure 1c is the spectrum of the solution containing 17 mM 4-ethylphenol and 25 mM CTAB (corresponding to $M = 0.66$). There is a clear line broadening and an upfield shift observed for the 4-ethylphenol peaks in the presence

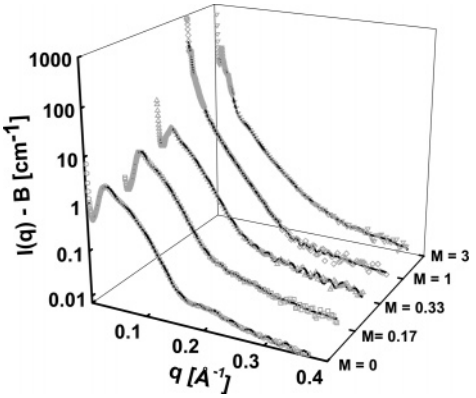

Figure 2. SANS profiles for CTAB micelles doped with varying concentrations of 4-ethylphenol (symbols) and the corresponding GIFT approximations (solid lines). M is the molar ratio of CTAB-to-4-ethylphenol. The CTAB concentration is 50 mM in all cases.

of CTAB. Hedin and co-workers[15] and Kreke and co-workers[29] have observed similar upfield shifts in the proton resonances upon the addition of an aromatic (benzene) or aromatic counterion (chlorobenzoate) into CTAB micellar solutions and ascribe such shifts to the insertion of aromatic rings into the micelle palisade. The line broadening is a consequence of restrictions to rotational motion on the NMR time scale and is further evidence of incorporation of 4-ethylphenol into the micelle structure.

SANS Analysis

SANS was employed to obtain information about the size and shape of the micelles and to investigate any evidence of phase transition upon loss of optical transparency in the system. Figure 2 illustrates the SANS scattering profiles for CTAB micelles doped with varying concentrations of 4-ethylphenol. The symbols in the scattering profile indicate the experimental data, and the solid lines indicate approximations by the GIFT technique using the structure factor calculations for charged spheres as detailed in the literature.[28] The first few data points (low q data) were not included in the GIFT calculations to avoid the effect of strong interparticle correlations.

The GIFT analysis of the SANS data yields the corresponding PDDFs that provide an understanding of the basic micellar shapes and size (Figure 3). For spherical scattering entities, the PDDF should be symmetrical, and the position where the curve intersects the r axis indicates the diameter of the sphere. In the case of cylinders, the PDDF is not symmetrical and the axial length of the cylinder is responsible for the linear region of $p(r)$ for large r. The distance at which the PDDF decays to zero provides a measure of the length.[27] Monodisperse vesicles ideally produce oscillations in the PDDF at large r values.[30] Such oscillations in the PDDF are smeared out in the case of polydisperse vesicles.[31] The largest particle size that can be measured accurately through GIFT is given by $d_{max} \leq \epsilon \pi/q_{min}$ ($d_{max} \approx 80$ nm in the present study). For particles bigger than d_{max}, no quantitative comparison should be made.[26]

With the exception of the data for very low q values, the approximations obtained by GIFT are in good agreement with the experimental data. Figure 3a shows the PDDFs for CTAB micelles doped with varying concentrations of 4-ethylphenol ($M \leq 1$). In the case of the control CTAB micelles ($M = 0$), a symmetric bell-shaped PDDF is observed, indicative of globular entities. The diameter of the micelles obtained through GIFT analysis (~6 nm, Figure 3a) is in good agreement with the value reported in the literature for the concentration of CTAB used in this study.[28] CTAB micelles doped with 4-ethylphenol, at $M = 0.17$, show indications of a structural transition with a small tail at larger distances, r. The symmetrical part of the PDDF suggests the presence of globular entities (micelles). The slight asymmetry at larger distances indicates the possibility of the coexistence of elongated micelle structures. Strictly speaking, the structure factor-model used for the GIFT calculations is valid only for spherical scattering entities. Thus, it is very difficult to obtain exact quantitative information on the size and distribution of the scattering entities once elongated micelles are present in the system. However, qualitative information on structural changes, such as sphere-to-elongated micelle transitions, can always be deduced from the shape change in the PDDFs. The PDDF for CTAB micelles doped with 4-ethylphenol, at $M = 0.33$, is indicative of rodlike/cylindrical scattering entities, implying that cylindrical micelles are predominant in the micellar system. This gradual sphere-to-cylinder transition, observed through the analysis of SANS data, has been noted in other SANS studies of other micellar systems involving CTAB and ionic dopants including KBr, KCl, and sodium salicylate.[11,28,32]

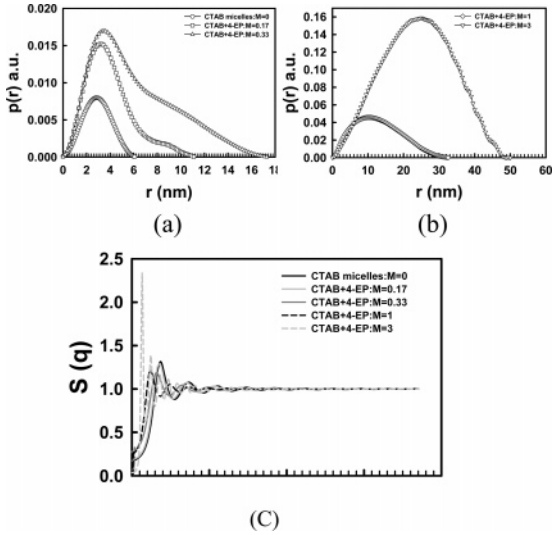

Figure 3. PDDFs for CTAB micelles doped with varying concentrations of 4-ethylphenol (M is the molar ratio of dopant to CTAB). The PDDFs are obtained through the GIFT analysis. (a) $M = 0-0.33$. (b) $M = 1$ and 3. (c) Structure factors (HNC closure relation) for CTAB micelles at various M values. [CTAB] = 50 mM.

In the case of CTAB micelles with concentrations of 4-ethylphenol corresponding to $M = 1$ and $M = 3$, the PDDFs are characteristic of large globular entities (Figure 3b). For the CTAB/4-ethylphenol system at $M = 1$, the PDDF does not indicate an unambiguous micellar shape. However, a system of polydisperse vesicles coexisting with a few elongated micelles is capable of producing the PDDF observed in Figure 3b. The PDDF of the CTAB/4-ethylphenol system at $M = 3$ (Figure 3b) exhibits a linear dependence on r for small distances, typical of a system comprised of lamellar entities (vesicles, disks, etc.).[30] The lack of oscillations at large distances (high r) reflects the polydispersity in the system. Figure 3c indicates that there are appreciable interparticle interactions present in these micellar systems. The interaction peak observed in the

(29) Kreke, P. J.; Magid, L. J.; Gee, J. C. *Langmuir* **1996**, *12*, 699.
(30) Glatter, O. *J. Appl. Crystallogr.* **1979**, *12*, 166.
(31) Iampietro, D. J.; Brasher, L. L.; Kaler, E. W. *J. Phys. Chem. B* **1998**, *102*, 3105.

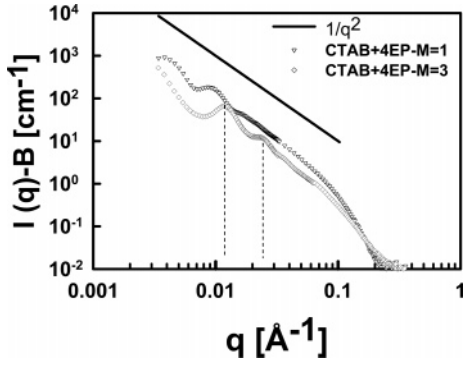

Figure 4. Scattering intensity after background subtraction vs wavevector, q on a log−log plot, the solid line represents a slope of −2, typical of lamellar scattering entities. The dotted lines indicate the peak positions for the scattering curve obtained from the $M = 3$ system. [CTAB] = 50 mM.

SANS data (Figure 2) and suppressed low-angle (q) scattering is due to these structure-factor effects. The structure-factor peaks in Figure 3c shift to smaller angles as the concentration of 4-ethylphenol increases progressively. This shift indicates that the scattering entities grow in size as the dopant is added to the micelles. The increase in the amplitude of the peaks indicates an increase in volume fraction of the scattering entities, but polydispersity leads to smoothing of the oscillations.[31,33] These oscillations appear smoothened in the case of $M = 0.33$ and $M = 1$ systems, possibly as a result of the polydispersity in these systems. At the length scales less than the dimensions of the scattering entities, interparticle interactions are not important (neutrons only "see" the structure of the individual particles); therefore, at large values of the scattering vector, q (which represents very small length scales in the real space), all the structure factors converge to unity.

Although SANS analysis does not offer conclusive information about the exact size of the scattering entities, the PDDFs indicate that the scattering entities progressively grow in size upon progressive addition of the dopant. In addition, the area under the PDDF is proportional to the aggregation number of molecules in a micelle. In the cases where $M = 1$ and $M = 3$, the aggregation number seems to be significantly larger than the aggregation number for CTAB micelles doped with lower dopant concentrations, further suggesting the possibility of the presence of larger self-assembled structures.

In Figure 4, the scattering intensity (after background correction) is plotted on a log−log scale. The straight line indicates a q^{-2} dependence of the scattering intensity ($I(q) - B$), typical of lamellar scattering entities, such as polydisperse vesicles and disks. The scattering curves for the $M = 1$ and $M = 3$ systems do reflect an approximate q^{-2} dependence. Another interesting observation for the $M = 3$ system is that two broad peaks characteristic of lamellar symmetry are also seen in the scattering curve (designated by the vertical dashed lines of Figure 4a at $q = 0.0118$ A^{-1} and $2q = 0.0234$ A^{-1}). The d spacing for such lamellar structures are on the order of 50 nm.

Cryo-TEM Analysis

Direct imaging cryogenic TEM (cryo-TEM) has emerged as an artifact-free method for observing diverse systems such as surfactant aggregates, polymer and polymer−surfactant solutions, microemulsions, and biological and biomedical systems.[34] These methods provide the ability to preserve microstructures by rapid vitrification of the solution containing the aggregates. In cryo-TEM, this is accomplished by forming a thin film of the sample on a specially prepared electron microscope grid, transferring the vitrified sample onto a cold stage without exposure to the environment and maintaining the sample temperature well below the amorphous-to-crystalline phase transition temperature during the imaging.

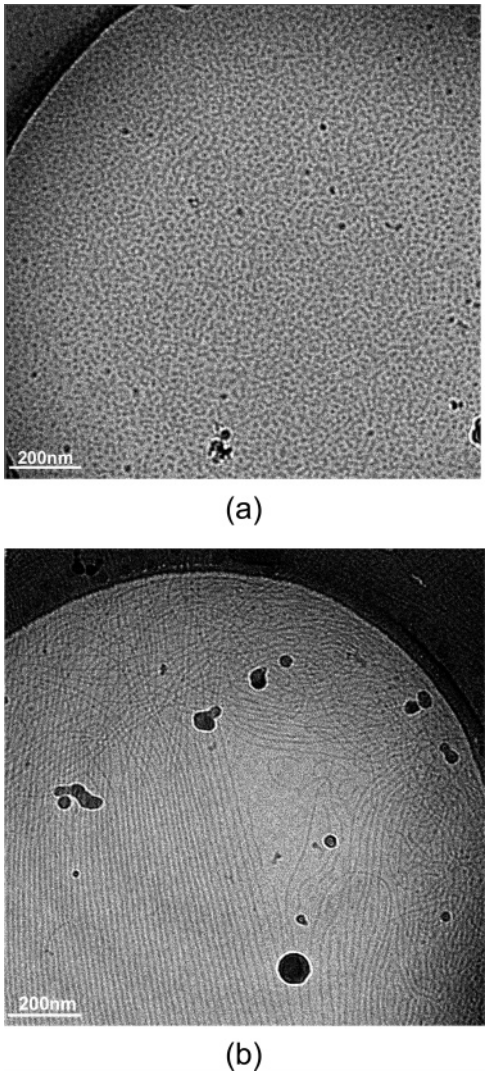

Figure 5. Cryo-TEM micrographs of CTAB micelles doped with 4-ethylphenol. (a) $M = 0$, spherical micelles are visible all over the grid, (b) $M = 0.33$, wormlike micelles are observed. [CTAB] = 50 mM.

CTAB micellar solutions containing varying dopant concentrations corresponding to $M = 0$, 0.33, 1.0, and 3.0 were analyzed using cryo-TEM. Figure 5a shows the cryo-TEM micrograph for the control CTAB micellar solution, $M = 0$. Spherical CTAB micelles are observed, consistent with the phase diagram for CTAB + H_2O binary system.[35] These spherical micelles are approximately 6−8 nm in diameter, in good agreement with the SANS analysis.

Figure 5b is an image of the CTAB/4-ethylphenol system at $M = 0.33$. Long wormlike micelles are seen throughout the sample, consistent with the SANS results. This is direct

(32) Aswal, V. K.; Goyal, P. S.; Thiyagarajan, P. *J. Phys. Chem. B* **1998**, *102*, 2469.
(33) Popela, J. B.; Glatter, O. *J. Appl. Crystallogr.* **1997**, *30*, 431.
(34) Danino, D.; Talmon, Y. In *Physical Chemistry of Biological Interfaces*; Marcel Dekker: New York, 2000; p 799.
(35) Waernheim, T.; Joensson, A. *J. Colloid Interface Sci.* **1988**, *125*, 627.

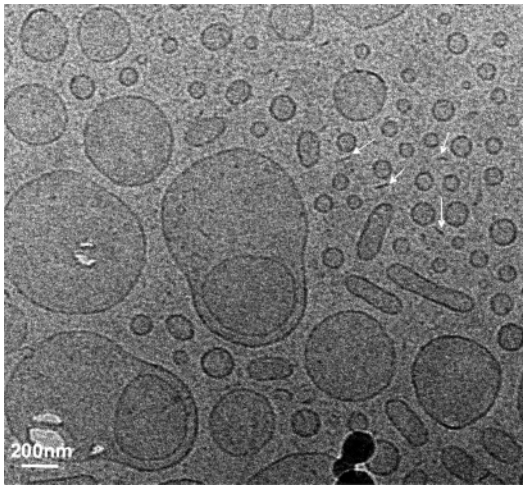

Figure 6. Cryo-TEM micrographs of CTAB micelles doped with 4-ethylphenol, $M = 1$, polydisperse vesicles are observed. The arrows show disks, which are the precusrsors to the vesicles. [CTAB] = 50 mM.

evidence that the progressive addition of 4-ethylphenol promotes micellar growth in the system. Thus, the addition of phenols to CTAB micelles leads to structural transitions that mimic the transitions observed when ionic hydrotropes are added to CTAB[8−11,36] and other cationic[37] and nonionic[38] surfactants. Our hypothesis is that CTAB headgroup repulsions may be decreased by the introduction of the polar dopant. The hydroxyl dipoles align to minimize the electrostatic field, effectively increasing the interfacial dielectric constant. Phenols have significant proton-donation tendencies, and the hydrogen-bonding affinity of these molecules may rigidify the interface leading to larger curvatures. Additionally, the hydrophobic part of the dopant increases the effective volume of the assembly tail region.

Interestingly, as the dopant-to-surfactant molar ratio is increased to $M = 1$, polydisperse vesicles are observed (Figure 6). In addition, disklike objects are also observed. Mixed micelles transform to bilayer disks as the dopant concentration is raised. When the disks reach a critical size, dictated by a balance between the bilayer bending modulus and edge energy, they fold up into vesicles.[39] Beyond these levels, 4-ethylphenol is not a dopant, but rather it is the major component of the system. The observation of vesicles reinforces the deductions on structure obtained through the SANS analysis. The cylinder (at $M = 0.33$) to vesicle transition (at $M \geq 1$) is fully evident at $M = 3$ (Figure 7a), where a considerable increase in the number of spherical vesicles is observed. In some cases, vesicles within vesicles are observed (Figure 7b). Also, oblong-shaped or tubular vesicles can be seen in Figure 7c. Tubular vesicles (L_{tv}), similar to the ones seen in Figure 7c, have been identified by Chiruvolu and co-workers in a ternary mixture of dimyristoylphosphatidylcholine (DMPC), water, and geraniol using cryo-TEM and optical microscopy.[17] While peaks indicative of a lamellar symmetry are present in the SANS curve for the $M = 3$ system (Figure 4a), it is not evident that the cryo-TEMs of Figures 7b and 8c indeed reflect lamellar structures with ~50 nm spacing. Nevertheless, it is clear

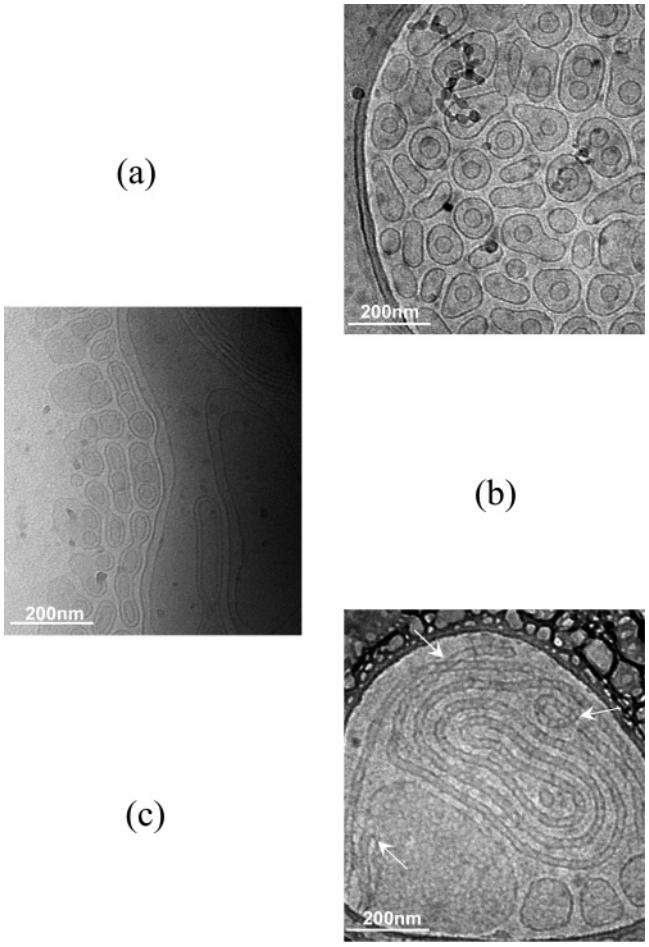

Figure 7. Cryo-TEM micrographs of CTAB micelles doped with 4-ethylphenol, $M = 3$. Polydisperse vesicles are present (a), along with vesicles embedded within other vesicles (b), entanglements, crossovers, and the evolution of a tubule structure from a large globular type vesicle structure can also be seen (c, arrows). [CTAB] = 50 mM.

that polydisperse but roughly spherical vesicles coexist with tubule structures. The tubule structure of Figure 7c shows entanglements, crossovers, and remarkably, the evolution of a tubule structure from a large globular-type vesicle structure (indicated by the arrows in Figure 7c).

In summary, the clear conclusion from both SANS and cryo-TEM is that the progressive addition of the phenolic dopant to the CTAB micelles leads to a systematic decrease in the micellar curvature. The micellar system is comprised of spherical micelles without the dopant. Three spherical micelles undergo transitions to elongated micelles upon incremental addition of the dopant, 4-ethylphenol. Disks that are precursors to vesicles are observed. When the 4-ethylphenol level reaches that of the cationic surfactant, vesicles are clearly observed, and when the 4-ethylphenol concentration is significantly in excess, extremely long tubelike vesicular structures are also seen, some of which protrude from large globular vesicles. It is hypothesized that, at these larger phenol concentrations, interfacial rigidity is enhanced by phenol hydrogen-bonding effects, thus leading to structures with low curvature. Recently, Won and co-workers[40] have reported a fascinating reverse transition, from bilayers to cylinders to spheres, in micellar systems of poly(ethylene oxide) (PEO)-based block copolymers. The reverse transition from spheres to cylinders

(36) Lin, Z.; Cai, J. J.; Scriven, L. E.; Davis, H. T. *J. Phys. Chem.* **1994**, *98*, 5984.
(37) Bernheim-Groswasser, A.; Zana, R.; Talmon, Y. *J. Phys. Chem. B* **2000**, *104*, 4005.
(38) Oberdisse, J.; Regev, O.; Porte, G. *J. Phys. Chem. B* **1998**, *102*, 1102.
(39) Lipowsky, R. *J. Phys. II France* **1992**, *2*, 1825.
(40) Won, Y.-Y.; Brannan, A. K.; Davis, H. T.; Bates, F. S. *J. Phys. Chem. B* **2002**, *106*, 3354.

to globular and tubular vesicles, as shown in this work, illustrates that such extensive microstructural changes can also be induced in small amphiphile systems.

Conclusions

We have investigated the effect of doping CTAB micelles with varying concentrations of a polar organic additive, 4-ethylphenol. Cryo-TEM and small angle neutron scattering techniques were employed to evaluate the effect of the 4-ethylphenol concentration on the shape and size of CTAB micelles. Interestingly, as the dopant concentration is increased, a transformation from spherical micelles to elongated micelles, to disks, and subsequently to globular and then to tubular vesicles is observed.

Doping with a polar organic additive offers a method of controlling the shape and the size of CTAB micelles. These micelles can then be used in the templated synthesis of mesoporous materials. Altering the structure of the micellar system that serves as a template for the synthesis of mesoporous materials may provide an easy route to tailor the structure and properties of the mesoporous materials.[24,41] CTAB micelles are integral to the synthesis of the M41S family of mesoporous silica.[20] In our recent work, we have found that the incorporation of phenolic dopants to these micelles can affect transitions from hexagonal to lamellar structures of ceramic materials synthesized in these systems.[24] It is important to note that the studies described here are not at very dilute surfactant concentrations but are at concentrations typically used in mesopore ceramic synthesis.[20]

Acknowledgment. We are grateful to Dr. Boualem Hammouda (NIST) and Dr. Lionel Porcar (NIST) for insightful discussions. Dr. Hammouda is also acknowledged for help in acquiring the SANS data. The National Institute of Standards and Technology, U.S. Department of Commerce, is gratefully acknowledged for providing the neutron research facilities used in this work through grant NSF/DMR-9986442. The work was supported by grants from the National Science Foundation (Grants 0092001 and 0329311) and NASA (NAG-1-02070). Disclaimer: NIST does not endorse equipment or chemicals mentioned in this paper.

LA048967U

(41) Pevzner, S.; Regev, O.; Lind, A.; Linden, M. *J. Am. Chem. Soc.* **2003**, *125*, 652.